Climatology and Interannual Variability of Cloudiness in the Atlantic Arctic from Surface Observations since the Late Nineteenth Century

ALEXANDER V. CHERNOKULSKY,[a] IGOR ESAU,[b] OLGA N. BULYGINA,[c] RICHARD DAVY,[b] IGOR I. MOKHOV,[a,d] STEPHEN OUTTEN,[b] AND VLADIMIR A. SEMENOV[a,e]

[a] *A. M. Obukhov Institute of Atmospheric Physics, Russian Academy of Sciences, Moscow, Russia*
[b] *Nansen Environmental and Remote Sensing Center, Bjerknes Centre for Climate Research, Bergen, Norway*
[c] *All-Russian Research Institute of Hydrometeorological Information—World Data Center, Obninsk, Russia*
[d] *M. V. Lomonosov Moscow State University, Moscow, Russia*
[e] *Institute of Geography, Russian Academy of Sciences, Moscow, Russia*

(Manuscript received 21 April 2016, in final form 16 November 2016)

ABSTRACT

A long-term climatology of cloudiness over the Norwegian, Barents, and Kara Seas (NBK) based on visual surface observations is presented. Annual mean total cloud cover (TCC) is almost equal over solid-ice (SI) and open-water (OW) regions of the NBK (73% ± 3% and 76% ± 2%, respectively). In general, TCC has higher intra- and interannual variability over SI than over OW. A decrease of TCC in the middle of the twentieth century and an increase in the last few decades was found at individual stations and for the NBK as a whole. In most cases these changes are statistically significant with magnitudes exceeding the data uncertainty that is associated with the surface observations. The most pronounced trends are observed in autumn when the largest changes to the sea ice concentration (SIC) occur. TCC over SI correlates significantly with SIC in the Barents Sea, with a statistically significant correlation coefficient between annual TCC and SIC of −0.38 for the period 1936–2013. Cloudiness over OW shows nonsignificant correlation with SIC. An overall increase in the frequency of broken and scattered cloud conditions and a decrease in the frequency of overcast and cloudless conditions were found over OW. These changes are statistically significant and likely to be connected with the long-term changes of morphological types (an increase of convective and a decrease of stratiform cloud amounts).

1. Introduction

As Earth warms steadily under climate change, nowhere are the effects of this warming more readily apparent than in the Arctic. This is a highly sensitive region where numerous processes combine to generate the so-called Arctic amplification (Pithan and Mauritsen 2014; Bekryaev et al. 2010; Serreze and Barry 2011). One of the important climate feedbacks is related to the role of clouds (Taylor et al. 2013). In the Arctic, clouds have a strong warming effect year-round except for a few weeks in the summer (Curry et al. 1996) with a sensitivity reaching 1 W m^{-2} per percentage of cloud cover (Shupe and Intrieri 2004). Arctic clouds also have a complex interaction with sea ice. By changing the radiative balance, cloud variability partially controls the sea ice albedo feedback by modulating the sea ice variability (Kay et al. 2008; Kay and Gettelman 2009; Kapsch et al. 2013; Choi et al. 2014; Liu and Key 2014), while the characteristics of those same clouds are partially determined by the sea ice variability (Vavrus et al. 2011b; Eastman and Warren 2010a; Palm et al. 2010; Sato et al. 2012; Heitzinberg et al. 2015).

The limited observational record is one of the major challenges in the assessment of Arctic clouds. The harsh conditions in the Arctic have limited spatial and temporal distribution of surface observations (both station based

Denotes content that is immediately available upon publication as open access.

Supplemental information related to this paper is available at the Journals Online website: http://dx.doi.org/10.1175/JCLI-D-16-0329.s1.

Corresponding author e-mail: Alexander Chernokulsky, a.chernokulsky@ifaran.ru

DOI: 10.1175/JCLI-D-16-0329.1

and ship based). Satellites have the potential to overcome this limitation, but satellite data only cover the period since the end of the 1970s (except Meteor satellite data, which started in the early 1970s; Mokhov 1991; Mokhov and Schlesinger 1993, 1994). However, there is a disagreement between different satellite observations and between the satellite and surface observations in both the climatology and the trends (Chernokulsky and Mokhov 2012; Stubenrauch et al. 2013; Eastman and Warren 2010b). Reanalyses also have biases in cloud characteristics, especially in winter and over the ocean (Chernokulsky and Mokhov 2012; Lindsay et al. 2014; Liu and Key 2016). The lack of reliable observations of clouds in the Arctic makes it challenging to validate climate models. Numerous studies have shown that global climate models have biases in their representation of clouds and cloud-radiation interactions (Jiang et al. 2012; Li et al. 2012; Komurcu et al. 2014; English et al. 2015; Karlsson and Svensson 2013). Thus, models fail to capture how clouds in the Arctic change in response to external forcings (English et al. 2015). To improve model representation of the variability of clouds in the Arctic, it is essential to validate these models with observations of both interannual and long-term variability (e.g., the early twentieth-century warming in the Arctic; Bengtsson et al. 2004).

This paper provides new insight into the variability of total cloud cover (TCC) based on long-term surface observations from Norwegian and Russian meteorological stations over the Atlantic sector of the Arctic [constrained to the Norwegian, Barents, and Kara Seas (NBK)]. The NBK region plays a central role in the Arctic climate system (Smedsrud et al. 2013). There was a drastic reduction of sea ice in the recent decade that resulted in almost ice-free conditions in the whole Barents Sea and parts of the Kara Sea (Smedsrud et al. 2013). These changes had a strong effect on regional and large-scale atmospheric circulation (Petoukhov and Semenov 2010; Outten and Esau 2012; Semenov and Latif 2015).

Section 2 of this paper provides a review of different aspects of clouds in the NBK, including their climatology and interannual variability. Section 3 presents a detailed description of the data and processing methodology, as well as their possible drawbacks. Section 4 provides an assessment of the climatology and variability of total cloud cover and the frequency of different cloud cover conditions in NBK. Section 5 summarizes the results and provides concluding remarks.

2. Cloudiness in the NBK region of the Arctic: A review

Cloud formation and evolution in the Arctic depends on a number of factors including large-scale atmospheric circulation, boundary layer structure, surface properties (sea ice and open water), and microphysical processes. The first analysis of long-term interannual variability of cloud cover in the Arctic (including NBK) was presented by Raatz (1981) and was based on polar-day observations from seven stations (two stations in NBK, Jan-Mayen, and Bjornoya) for the period of 1921–78. A more comprehensive analysis of cloud cover and cloud type interannual variability over the Arctic was done by Eastman and Warren (2010a), who used visual observations from land stations, ships, and drifting stations for the period of 1971–2007. In general, the agreement among different datasets for TCC is the highest in the Norwegian and Barents Sea regions of the Arctic (Chernokulsky and Mokhov 2012).

Several important peculiarities of the NBK region include the highest surface skin temperature in the Arctic (Wang and Key 2005a), relatively low sea ice fraction (Smedsrud et al. 2013), and the lowest mean sea level pressure with the highest cyclone frequency in the Arctic (Akperov et al. 2015). The combined effect of these makes this region among the cloudiest in both the Arctic and the world (Table 1) (Mokhov and Schlesinger 1994; Chernokulsky and Mokhov 2010; Liu et al. 2012a; Karlsson et al. 2013; King et al. 2013; Stubenrauch et al. 2013).

Total cloud cover in the NBK region varies from 80% to 100%.[1] Over the Norwegian and Barents Seas, there is only a weak annual cycle of TCC. Over the Kara Sea there is a maximum in TCC in August–September according to various satellite and surface observations (Chernokulsky and Mokhov 2012). This summertime maximum comes from warmer temperatures and greater moisture availability over the melting sea ice (Herman and Goody 1976). TCC in NBK has significant correlation with surface air temperature (the correlation is negative in summer and positive in winter) (Warren et al. 2007) and sea surface temperature (positive correlation in all seasons) (Eastman et al. 2011). Interannual variability of cloudiness characteristics in NBK is controlled by atmospheric circulation (Mokhov et al. 2009; Zhang et al. 2012; Chernokulsky et al. 2013; Bednorz et al. 2016), particularly by the position of cyclone tracks in the winter and the strength of anticyclones in the summer (Bednorz et al. 2016). The North Atlantic Oscillation (NAO) modulates the transport of moisture into the NBK region

[1] For clarity, where percentages are quoted throughout this work, they refer to absolute percentage cloud cover of the total sky. For example, 80% cloud cover means 80% of the sky is covered with clouds, while a 20% reduction in this cloud cover would reduce it to 60%.

(Smedsrud et al. 2013). Previdi and Veron (2007) showed that the positive phase of the NAO is associated with positive anomalies of cloud water path, mostly because of liquid water path.

Cloudiness in the NBK region is mostly from stratiform clouds of all levels (Hahn and Warren 2007; Eastman and Warren 2010a; Liu et al. 2012a; Esau and Chernokulsky 2015; Li et al. 2015), with low-level clouds occurring the most frequently (Curry et al. 1996; Liu et al. 2012a). Low-cloud properties depend mostly on local evaporation from the Arctic Ocean and consequently depend on sea ice conditions (Eastman and Warren 2010a; Palm et al. 2010; Vavrus et al. 2011a), whereas mid- and high-level cloud changes are mostly driven remotely via changes in meridional moisture transport from lower latitudes (Vavrus et al. 2011a; Zhang et al. 2012). The prevalence of stratiform clouds over NBK is attributed to the northeastward advection over the cold sea ice surface of moist relatively warm air that forms in the North Atlantic (Herman and Goody 1976).

Advection of cold air (so-called cold-air outbreaks), which is common for the NBK (Kolstad et al. 2009), triggers unstable atmospheric conditions and the presence of convective cloudiness and thunderstorms in the Atlantic sector of the Arctic (Brümmer and Pohlmann 2000; Czernecki et al. 2013; Esau and Chernokulsky 2015). Czernecki et al. (2013) have found that thunderstorms in the Norwegian Sea can also be associated with warm moist advection in the middle atmosphere during summertime; however, these thunderstorms are characterized by weaker convective instabilities than those induced by cold air outbreaks. Convective cloudiness in NBK [cumulus (Cu) and cumulonimbus (Cb)] takes place in all seasons with a weak annual cycle (Esau and Chernokulsky 2015). It varies from a few percent in the northeast (over sea ice) to 10%–15% (up to 30% in some years) in the southwest (over open water). It has also been suggested that the convective self-organization of cumuli clouds into cloud cells and rolls (cloud streets) might intensify polar storms (Okland 1987).

The amount of stratus (St) and stratocumulus (Sc) clouds combined reaches 50% according to surface observations (Esau and Chernokulsky 2015) and 60% according to satellite observations (Li et al. 2015). Stratocumulus clouds are the most common of the morphological types, including stratus clouds, reaching around 30% of the TCC (Wood 2012; Esau and Chernokulsky 2015). A maximum in stratocumulus clouds occurs in August and is most prominent in the Kara Sea (Wood 2012). Multilayered stratiform clouds account for up to 40% of the TCC (Mace et al. 2009; Liu et al. 2012a; Li et al. 2015), which tend to have minimum-random overlap (Li et al. 2015). Multilayered clouds in NBK are mainly a result of the overlap of low-level stratiform clouds with altostratus (As) clouds (Li et al. 2015), which have a horizontal dimension of 300 km in winter and spring and 400 km in summer and autumn (Wood and Field 2011).

The diurnal cycle of TCC is not generally well defined according to both surface (Eastman and Warren 2014) and satellite (Wylie 2008; King et al. 2013) observations, with a diurnal amplitude of TCC not exceeding 3%–5% (Wylie 2008; Eastman and Warren 2014). The morning maximum of low-level cloudiness is dominated by the occurrence of stratocumulus clouds in NBK (Eastman and Warren 2014).

Przybylak (1999) estimated cloudiness changes from eight stations in NBK (combined with four stations in Siberia) for the period 1951–90. He found a statistically significant increase in winter and annual means of TCC with a linear trend of 2.6% decade^{-1} in winter and 0.8% decade^{-1} for the whole year. For TCC, a positive linear trend was found for the western part of NBK (about 0.9% decade^{-1} in autumn and 0.5% decade^{-1} in other seasons). For the eastern part of NBK (east of 40°E), TCC was found to increase only in autumn (with a linear trend of 0.8% decade^{-1}) and decrease in other seasons, with the most pronounced negative trend in spring (-3.6% decade^{-1}). This reduction is accompanied by an increase of clear sky frequency (trend of 0.028 decade^{-1}), whereas in other seasons, and over the western part of NBK for the whole year, clear sky frequency changes are nonsignificant (Eastman and Warren 2010a). Similar trends of TCC were found for winters over the last 20 years from satellite (Advanced Polar Pathfinder) and reanalysis (ERA-40) data (Liu et al. 2008), with positive trends over the western NBK and negative trends over the eastern NBK, associated with a corresponding increase and decrease of moisture convergence. The increase of TCC in the Barents Sea leads to an increase of downwelling longwave radiation flux (with a linear trend of up to 10 W m^{-2} decade^{-1} (Francis and Hunter 2007) and a decrease of incoming solar radiation (Stanhill 1995). However, satellite- and surface-based observations do not agree well when assessing year-to-year cloud variability and show nonsignificant correlation in autumn and winter over sea ice regions (Eastman and Warren 2010b) (Table 1).

Changes in TCC are mainly associated with changes in the amount of stratocumulus cloud (the most common form of clouds in the NBK). The amount of stratocumulus cloud increases in the western part of the NBK (with a linear trend of around 1%–2% decade^{-1} in all seasons) and decreases in the eastern part of the NBK (with linear trends down to -3.9% decade^{-1} in spring and -5.0% decade^{-1} in winter) except in the autumn when it increases with a 1.5% decade^{-1} trend

TABLE 1. The main characteristics of clouds in the Norwegian, Barents, and Kara Seas compare to the entire Arctic and global means (from published literature and available datasets).

Characteristic of clouds	The Atlantic Arctic		The Arctic	Global
	Values	Data and reference		
		Macrophysical characteristics		
Total cloud cover	Western part: 90%–100%, weak annual cycle Eastern part: 80%, late summer maximum	Seven satellite and one surface-based datasets Chernokulsky and Mokhov (2012)	65%–75% (Chernokulsky and Mokhov 2012)	65%–70% Chernokulsky and Mokhov (2010); Stubenrauch et al. (2013)
Amount of the main morphological type	Stratocumulus (25%–30%) with minimum in winter	ship-based (1954–2008) and station-based (1971–2007) data Eastman and Warren (2010a) station-based (1936–2013) data Esau and Chernokulsky (2015)	Stratocumulus (24%) Eastman and Warren (2010a)	Cirriforms (land) (22%) and Stratocumulus (ocean) (22%) Eastman et al. (2011)
	Stratus and Stratocumulus (60% in NB, 40% in K)	Active satellite radar-lidar observations (2007–10) Li et al. (2015)		
Multilayered cloudiness	30% from TCC	Active satellite radar-lidar observations (2007–10) Liu et al. (2012a)	26% from TCC Liu et al. (2012a)	25%–28% from TCC Li et al. (2015)
Dominant multiple cloud types	Altostratus + stratus/stratocumulus	Active satellite radar-lidar observations (2007–10) Li et al. (2015)	Altostratus + stratus/stratocumulus Li et al. (2015)	Cirriforms + Stratus/stratocumulus Li et al. (2015)
		Long-term variability and trends		
Total cloud fraction	Western NBK: positive trends in all seasons (0.5%–0.9% decade^{-1}) Eastern NBK: negative trend in all seasons (down to −3.6% decade^{-1} in spring) except for autumn (0.8% decade^{-1})	Ship- and station-based (1971–2007) data Eastman and Warren (2010a) In addition, for winter: passive satellite observations (1982–2000) and reanalysis (1982–2000) Liu et al. (2007)	Surface observations (1971–2007): positive trends in all seasons (0.2%–0.5% decade^{-1}) Eastman and Warren (2010a) Satellite observations (1982–2000): positive trends in spring and summer (0.2%–0.3% decade^{-1}) and negative trends in winter and autumn (down to −0.6% decade^{-1}) Wang and Key (2005b)	Surface data: negative trend over land and positive trend over the ocean Eastman et al. (2011); Eastman and Warren (2013) Satellite data: no significant concordant trends based on different satellite datasets Stubenrauch et al. (2013)
	Correlation of annual-mean TCC from surface and satellite data is around 0.5–0.7 over open water and around 0.2 over icy regions (with zero correlation in winter and autumn)	Surface and passive satellite observations (1982–2004) Eastman and Warren (2010b)	Surface and satellite observations (1982–2004): no correlations of TCC in its interannual variability in winter and autumn Eastman and Warren (2010b)	

TABLE 1. (*Continued*)

Characteristic of clouds	The Atlantic Arctic		The Arctic	Global
	Values	Data and reference		
Morphological types	Sc: increase in west and decrease in east of the NBK St: increase in east of the NBK in winter and spring Cu: increase in west of the NBK in summer and autumn Ns + Cb: decrease	Ship- and station-based (1971–2007) data Eastman and Warren (2010a)	St, Sc, Cu: increase Cb, Ns: decrease Eastman and Warren (2010a)	Land: Sc + Cu + Ac: positive trend St + Ns + As + high level: negative trend Cb: no trend Eastman and Warren (2013)
	Cu + Cb: increase over open-water regions St + Ns: decrease	Station-based (1936–2013) data Esau and Chernokulsky (2015)		Ocean: Low-level (St + Sc and Cu) and high-level cloud types: positive trend Ac + As: almost no trend Eastman et al. (2011)

(Eastman and Warren 2010a). The amount of stratus cloud increases only in the cold seasons (winter and spring) over the eastern part of NBK (with a 1.5% decade^{-1} linear trend). The amount of cumulus cloud increases in the warm part of the year (summer and autumn) over the entire NBK region with a trend of around 1% decade^{-1}. Positive trends were also noted for altostratus and high-level clouds (except in winter); however, for altocumulus (Ac) clouds there is a general negative trend. Additionally, a prominent reduction of precipitating clouds [cumulonimbus and nimbostratus (Ns)] has been observed over the last 40 years (with a linear trend of around −2.0% decade^{-1}), mostly because of a decrease in the amount of cumulonimbus clouds (Eastman and Warren 2010a). Esau and Chernokulsky (2015) analyzed data from 27 Russian weather stations in the Barents and Kara Seas for a longer period, 1936–2013. They found an increase in the amount of convective clouds over open-water regions with the most pronounced trends in autumn and winter (up to 0.7% decade^{-1}) and nonsignificant changes over sea ice covered regions. A reduction in the amount of strati and nimbostrati clouds was found over open water and sea ice–covered regions in all seasons except summer, with negative trends down to −2.0% decade^{-1} (Esau and Chernokulsky 2015).

Results of the reviewed studies indicate the absence of information on cloudiness in the NBK in the early years of observations (before the 1950s). It is particularly unclear how clouds behaved during the early twentieth-century warming when surface air temperature and sea ice concentration in NBK was similar to how it is today (Bengtsson et al. 2004; Zhichkin 2015). This paper provides a new insight into the variability of total cloud cover based on long-term surface observations from Norwegian and Russian meteorological stations for a period longer than is currently available. Analysis is presented from the end of the nineteenth century. This analysis allows for the assessment of contemporary trends in cloud characteristics with respect to past variations.

3. Data description and processing

a. Surface cloud observations

The analysis presented here is based on routine visual surface observations from the Norwegian and Russian coastal and island meteorological stations located in the NBK region (Fig. 1; supplementary Table S1). Reports from these stations are collected in the Norwegian Meteorological Institute (hereinafter eKlima data, available on the website eklima.met.no) and in the All-Russian Research Institute of Hydrometeorological Information

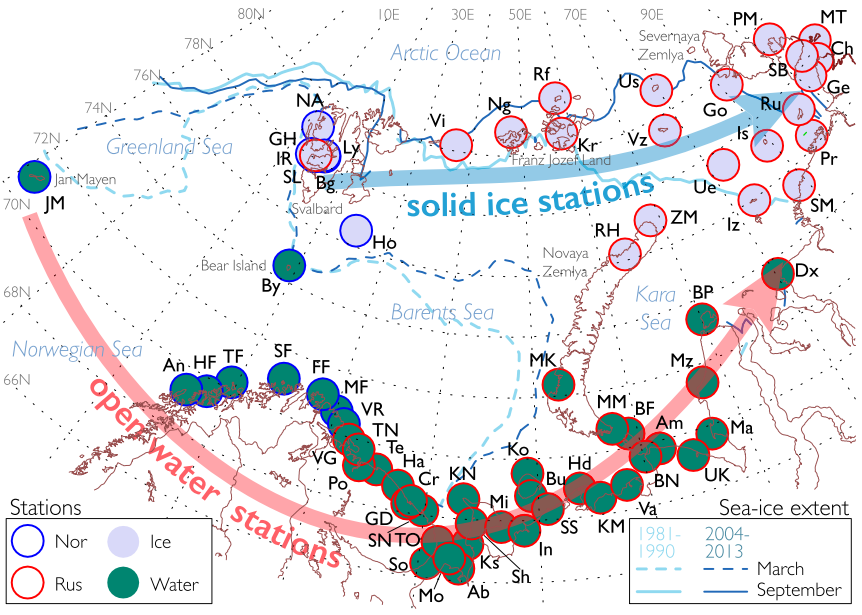

FIG. 1. Location of Norwegian (blue-rimmed circles) and Russian (red-rimmed circles) weather stations used in this study (see also supplementary Table S1). Stations with open-water conditions are shown by the green circles, stations with solid-ice conditions are shown by the blue circles. The boundaries for March (dashed lines) and September (solid lines) sea ice extent based on HadISST data (Rayner et al. 2003) are shown for the years 1981–90 (light blue lines) and 2004–13 years (dark blue lines).

(RIHMI; Bulygina et al. 2014; Chernokulsky et al. 2011, 2013), respectively.

We divided all the stations into two groups depending on ice conditions, which are defined based on the Hadley Centre Global Sea Ice and Sea Surface Temperature dataset (HadISST; Rayner et al. 2003). The first group includes stations with mostly open water surrounding (OW; the Norwegian Sea, the south coast of the Barents Sea, and the southwestern coast of the Kara Sea). Weather stations from the second group are located in mostly solid-ice conditions (SI; Svalbard, the islands from the northern part of the Barents and Kara Seas, and the southeastern coast of the Kara Sea) (Fig. 1). The division is tentative because of the seasonal variability in the sea ice extent. So in part of the OW (especially in the eastern NBK) sea ice is present during the intra-annual maximum, while a part of SI is free from sea ice during the intra-annual minimum. The interannual variability of sea ice extent also affects how we define the surroundings of the stations. In particular, the islands in the Kara Sea were surrounded by year-round ice before the 1990s but have become partly opened in recent years (Fig. 1). In addition, it is important to bear in mind that only data from surface stations are used (not from ship observations); thus it is hard to completely exclude the possible influence of land on cloud cover observations. However, the predominant role of large-scale processes and the sea ice boundary position on cloud formation in the NBK (see section 2 for more details) make this influence somewhat unimportant.

In total, we used information from 15 Norwegian and 54 Russian weather stations, which operate or operated in the NBK (Fig. 2; supplementary Table S1). None of these stations were relocated during the period of operation.

The paper is mainly focused on an analysis of TCC. It is identified by an observer from a visual inspection of the sky above a weather station and defined as the ratio between the cloudy part of the sky and the full sky. Originally, information on TCC was reported in oktas for the eKlima data and in tenths for the RIHMI data. In recent years measurements at the Norwegian stations were conducted four times a day, whereas in Russia observations are conducted eight times a day. During the twentieth century there were a number of changes in the timing of observations (Fig. 2), as well as the number of operating stations, from only 1 station at the end of the 1860s to 60 stations in the 1980s. The combined effect of these changes to observational practice resulted in large changes in the total number of cloud observations per year in the NBK n_{obs} (these changes are described in full in the supplementary material).

There were several shifts in observational procedures at both Russian and Norwegian stations. In Norway, starting from 1949, observers started to measure TCC in

oktas instead of tenths (Henderson-Sellers 1992). This led to a couple of issues for the consistency of observations: First, this transition led to observers retraining, which may have introduced mistakes in determining the actual cloud cover in a new system of units. And second, there may have been errors in converting the observations for the archives (Henderson-Sellers 1992). In particular, we found that the initial cloud data in eKlima for Bjornoya and Hopen islands contained errors for several years after the tenths-to-oktas transition. The removal of these errors is explained in the supplementary material.

There have also been several changes documented in the Russian observational procedure. In the nineteenth century and the first quarter of the twentieth century only total cloud cover was observed and recorded in the archive. At the end of the 1920s observers started to measure low cloud cover as well. Information about morphological cloud types appeared after 1936. From the beginning of the 1930s, cloud breaks (when TCC is more than 9 tenths but the sky is not completely overcast) and cloud traces (any nonzero cloud cover less than 1 tenth) were starting to be reported (in practice, a special code for cloud traces is used only at 16 out of 54 stations and only after 1983). There are no details as to how these cases were coded in the earlier period. Such shifts in observing practice may have affected the reported frequency of clear and overcast skies (Free and Sun 2013). There is no documented information on such changes for the Norwegian stations; however, we cannot exclude their possible presence in the first half of the twentieth century. For now, cloud traces and cloud breaks are treated as 1 and 7 oktas at Norwegian stations.

There is a chance of the presence of some undocumented changes in observational procedure in the data, which may impact on the time series homogeneity. Even the replacement of one observer with another who had a different training may influence the results, particularly on the identification of morphological cloud types (Eastman and Warren 2013). In all likelihood, the training of observers has improved since the nineteenth century, for instance, after the advent of air traffic (Henderson-Sellers 1992) and after the establishment of the World Weather Watch program. Consequently, the earlier records of cloud observations may be less reliable than contemporary observations.

b. *Data processing*

In this study, the major results are based on an analysis of seasonal means of TCC and the frequency of different morphologies of clouds, which are calculated based on the following steps and assumptions (the supplementary material provides more detailed information on the assumptions involved):

(i) To homogenize different observational measures (tenths in Russia/USSR and oktas in Norway), we converted all Russian data into oktas following the WMO guidelines (Table S2) for counting TCC. To keep an agreement between Russian and Norwegian data, we recalculated all cloud breaks into 7 oktas and presented these results in the main part of the paper. In the supplementary material, we presented results of an additional analysis for time series with cloud breaks considered as overcast. Cloud traces were treated as zero.

(ii) To reduce the uncertainty in the nighttime observations due to a lack of illumination, all reports were required to fulfill a moonlight criterion (Hahn et al. 1995). This criterion filters out observations that were made during dark nights; the threshold for the solar angle is 9° below the horizon, and the threshold for the relative lunar illuminance (which takes into account the phase and the height of the moon) is 0.11 (Hahn et al. 1995). About 25% of all reports were excluded as a result of the application of this criterion (up to 70% of reports during the polar night) (see Fig. 2).

(iii) All reports that satisfied the illuminance criterion were recalculated to monthly mean TCC by a simple averaging (with equal weights) and presented in percentage. Therefore, our results are more representative of daytime cloudiness. However, this simple averaging is a reasonable assumption owing to the near absence of a diurnal cycle of TCC in the NBK. Monthly means were recalculated to seasonal means. We used the one-month-shifted calendar for seasons, so winter mean is a mean for January, February, and March. Because some stations have sporadic gaps in observations with a somewhat uniform distribution in time, we calculated monthly means only if there were at least 10 days in the month with observations (no matter how many reports were made per day); otherwise the monthly mean was assigned as undefined. Seasonal means of a particular year were calculated if at least two monthly means were defined. Therefore seasonal means were calculated from at least 20 observation reports.

(iv) Because of possible observer-related uncertainties in the identification of the exact value of TCC, we calculated frequencies for four broad ranges of cloud cover: 1) cloudless conditions (CLR) when TCC was reported as zero or 1 okta (which allows us to directly compare Norwegian and Russian observations despite the possibility of different treatments of cloud traces), 2) scattered clouds (SCT) for $2 \leq \text{TCC} \leq 4$

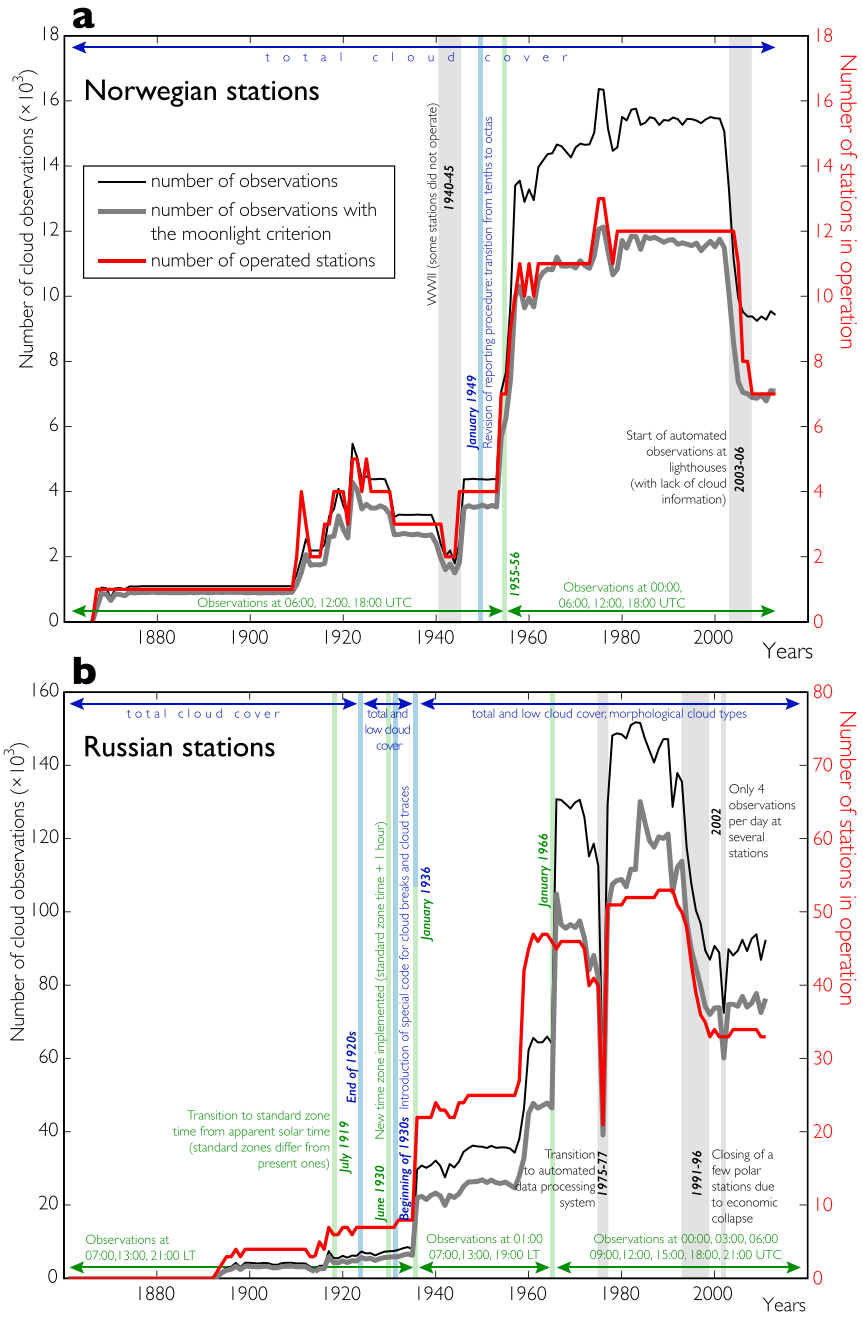

FIG. 2. Number of stations and number of cloud observations per year (with and without the moonlight criterion) from (a) Norwegian and (b) Russian stations, along with key changes in these observations. Time of observations and its changes are shown in green. Observation variables and changes in observational procedures are shown in blue. Other changes are shown in gray/black.

oktas, 3) broken clouds (BKN) for $4 < \text{TCC} \leq 7$ oktas, and 4) overcast conditions (OVC) for reported TCC of 8 oktas. The seasonal mean of these values is defined as a ratio of the number of reports with a given cloud cover to the total number of reports.

(v) The maximum systematic bias in the seasonal means of TCC, associated with the influence of changes in the timing of observations, the transition from reporting tenths to oktas, and issues with cloud traces/cloud breaks, is estimated to be within 5% (the procedure of bias estimation is given in the supplementary material, including Fig. S1). For CLR and SCT this bias is 5%, and for BKN and OVC it may reach 10%. These biases should be accounted for

when cloudiness changes at individual stations are analyzed. This is especially true for the early years, when changes of technique and timing of observations were frequent. For the period after 1936, when the special codes for cloud breaks and cloud traces had been implemented, the systematic bias does not exceed 2%–3% for TCC, CLR, and SCT and 5% for BKN and OVC.

(vi) To overcome the temporal inhomogeneity associated with variability in the number of stations we analyzed cloud variations for each individual station. The averaging for the entire region was carried out only for the period after 1936 when the number of stations in operation was sufficiently increased and systematic biases decreased. To avoid the possible influence of dropping or including systematically more cloudy or cloudless stations, the averaging was prepared in the following way: 1) the means of cloud characteristics were counted for each station (and for the entire region) for the period 1981–90 [this reference period was chosen as it was the period when almost all stations were in operation (24 stations for SI and 36 for OW)]; 2) anomalies relative to the corresponding mean in this reference period were taken for each station and for every year; 3) for every year, anomalies were averaged between stations that operated in that year; 4) the resulting values of the cloud characteristics for each year were obtained by adding the entire-region mean for the reference period to the average anomaly of the given year. Note that for regional averaging, anomalies for all operating stations were first averaged in each 10°-longitude sector (with equal weights), and then anomalies of 10° sectors were averaged (with equal weights) for the entire region. This was done to account for the spatial heterogeneity of the station locations.

(vii) Statistical significance of linear trends and correlation coefficients was calculated using the Student's *t* test while accounting for autocorrelation (with 1-yr lag) in effective sample size computing (Bartlett 1935).

4. Results

a. Cloudiness variability at individual stations

We use Hovmöller diagrams (Fig. 3) to show the year-to-year changes of TCC at individual meteorological stations in the NBK separately for different seasons and two distinct regions (SI and OW).

Over SI, the highest values of TCC are found in summer, especially over islands in the Barents and Kara Seas (TCC is around 90%) (Fig. 3a). For Svalbard, TCC is less (around 80%). The difference between the TCC over Svalbard and over the Barents and Kara Seas is also prominent in spring (60%–65% vs 70%–75%, respectively). The minimum values of TCC are found in winter (around 60%) (Fig. 3a). In autumn, TCC at most of the stations over SI is around 60% (Fig. 3g). The cloudiest SI station is Zhelaniya Mys (annual TCC is 79%). The absolute maximum and minimum for TCC and for other cloud characteristics can be found in the supplementary material (Table S3).

TCC is comparatively high in all seasons over OW, especially in summer and autumn (up to 80%–90% for particular stations) (Figs. 3f,h), but TCC is also relatively high at most of the OW stations in other seasons as well (around 70%–80%). Jan Mayen and Biornoya are the cloudiest stations in the entire NBK with TCC annual means of 83% and 82%, respectively. The minimum of TCC is found in the eastern part of the NBK in winter where it drops to 50% (Fig. 3b).

Several particularities of TCC interannual variability can be seen from these observations. First of all, there is a high year-to-year variability of TCC at the end of the nineteenth century and the beginning of the twentieth century. TCC at the first operating stations is reported to have varied from one year to another by more than 20%–30% (e.g., from 60% to 90%); moreover, neighboring stations display almost zero or even negative correlation of TCC anomalies from year to year. This may point to an overall low quality of cloud cover observations in the beginning of the era of meteorological observations in the NBK. From the 1930s onward, the correlation of TCC among neighboring stations became positive and significant. In the 1930s–50s, an overall increase of TCC is noted for all seasons over both SI and OW (except for winter over SI). Whereas in the 1960s–80s TCC decreased at almost all stations. In autumn, the decrease of TCC during this period exceeded 20% at several stations. In the 1990s TCC started to increase again, especially strongly in autumn. In general, higher interannual variability is reported for stations and periods where and when the highest variability of sea ice extent was observed. Spurious increases of TCC in the beginning of the 1990s (and then a decrease in the beginning of 2000s) at Chelyuskin Mys (Figs. 3a,g) are not supported by any of the neighboring stations. We therefore conclude they are likely to be artificial and not associated with environmental changes.

Among the different cloud conditions, the least common conditions are the CLR and SCT categories. CLR is especially rare over OW where it changes from 0.05–0.1 at the west stations to 0.1–0.2 at the east stations

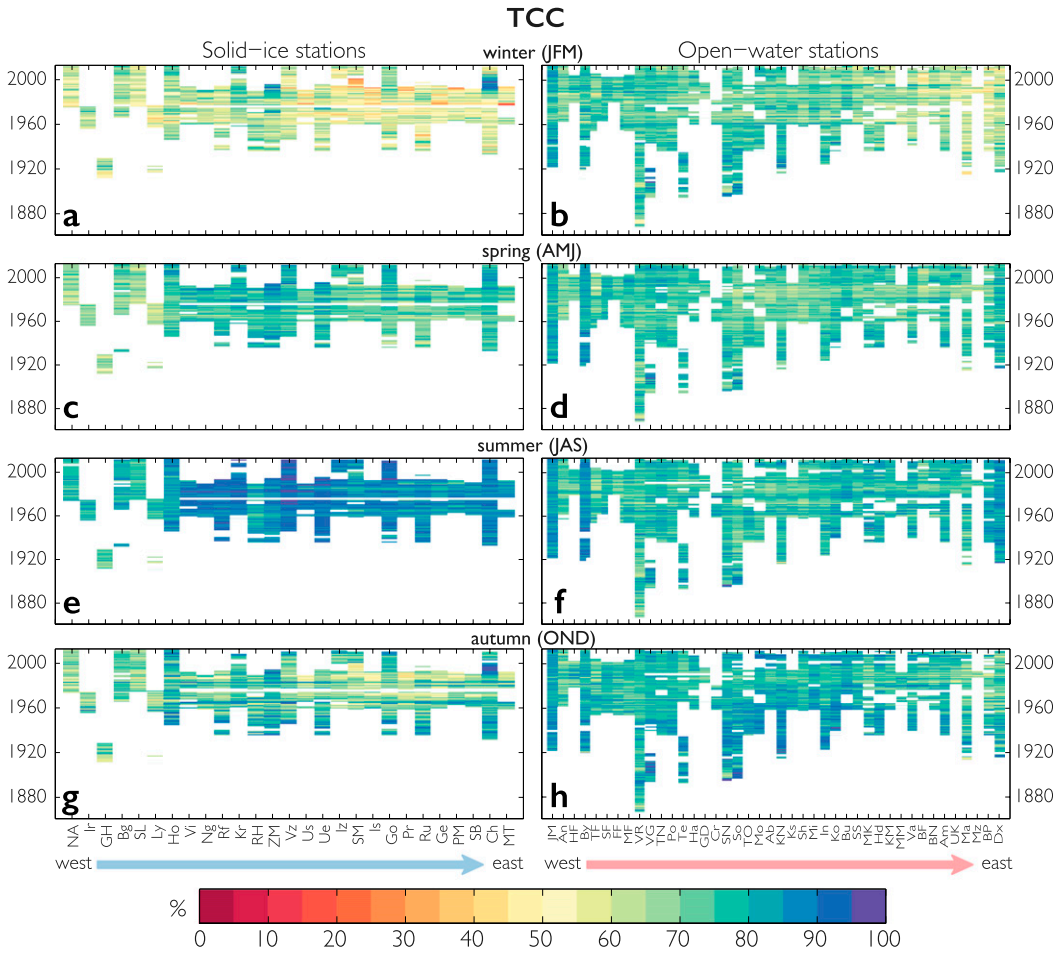

FIG. 3. Changes of total cloud cover in percent over (a),(c),(e),(g) solid-ice and (b),(d),(f),(h) open-water stations for (a),(b) winter, (c),(d) spring, (e),(f) summer, and (g),(h) autumn. Cloud breaks are considered as 7 oktas. Stations are ordered by longitude from west to east.

(see supplementary Fig. S3). The highest values of CLR (0.3–0.4) appeared mostly in winter over the southwestern coast of the Kara Sea (Fig. S3b). Over SI, annual-mean CLR varies from 0.1 to 0.2 and shows a pronounced annual cycle with the maximum in winter (0.25–0.35) and minimum in summer (around 0.05). In general, the highest values of CLR were observed over SI in the 1960s–80s, and mostly in winter (0.4–0.6) (Fig. S3a). A general decrease of CLR over SI has been found in the following years (1990s–present).

Scattered clouds are common for Svalbard where they were found in 13%–18% of all cases (Fig. S4). For other SI regions, annual mean of SCT varies around 0.1. In the Barents and Kara Seas the lowest values of SCT are found in summer (0.04–0.07), while in winter SCT may reach 0.2. Over OW, annual means of SCT do not show longitudinal dependence and they vary between around 0.1–0.15 with the minimum in autumn and winter (Fig. S4h). A little year-to-year variation of SCT (with a general increase from the 1930s) is found for both SI and OW stations.

Broken clouds are common for the NBK, especially for OW (Fig. S5). Annual means of BKN over OW vary between 0.3 and 0.5 and reach 0.6 for particular stations. In the eastern part of the NBK, BKN is as low as 0.25–0.3. BKN over OW has a weak annual cycle (Figs. S5b,d,f,h) but exhibits large interannual variability. BKN was notably lower at the end of the nineteenth century and at the beginning of the twentieth century according to both Norwegian and Russian observations. BKN slowly increased after the 1930s until the present day. BKN has a weak annual cycle over SI with the minimum in winter (Figs. S5a,c,e,g). In the Barents and Kara Seas, BKN is comparatively small and varies between 0.15 and 0.2. In the cold period of the 1960s, BKN increased up to 0.25–0.3. BKN is also generally higher over Svalbard (around 0.3–0.4). The highest values of BKN are observed at Svalbard Lufthavn, where the long-term annual mean is

0.50. Svalbard Lufthavn is the only airport station in our analysis, and it should be noted that observers for aviation purposes may quantify overcast situations in a different way. This may result in an overestimation of BKN (Figs. S5a,c,e,g) and underestimation of OVC (Figs. S6a,c,e,g) compared to the neighboring stations. Therefore, this station may not have sufficient consistency with other stations for the purposes of assessing cloudiness changes over Svalbard.

Overcast conditions are the most common among the other cloud conditions over SI in the NBK (Fig. S5). It is especially common in the Kara Sea where its annual means vary between 0.5 and 0.6 and summer means reach 0.8–0.9 (Fig. S6e). High values of summer OVC were also observed in the 1930–40s. However, overcast cases decreased by 0.1–0.2 in the cold period of the 1960–70s. Over Svalbard, OVC is markedly lower, with an annual mean of around 0.4, and 0.17 for Svalbard Lufthavn, and there was not such a decrease in OVC conditions during the 1960–70s. Over OW, OVC and BKN are comparable. The highest values of OVC were observed in the beginning of the twentieth century, when it reached 0.8–0.9 (Figs. S6b,d,f,h). However, the overall low quality of early period observations should again be emphasized. After the 1940s there was a general decrease of OVC for most of the OW stations. At the present time it varies around 0.4 with a weak annual cycle.

The treatment of cloud breaks as overcast results in somewhat higher values of TCC (around 1%–2%), higher values of OVC (around 0.05–0.1), and lower values of BKN (around 0.05–0.1) over Russian stations (Figs. S7–S9). However, the main features of spatio-temporal variations of TCC remain similar to those presented in Fig. 3, with a minimum in the 1960s–70s and two maxima in the 1930s–50s and in the last decades. BKN (OVC) shows a steady increase (decrease) over SI and OW stations starting from the 1930s.

b. Cloudiness variability in the entire NBK region

In this section, cloudiness for the entire NBK is analyzed for SI and OW. Table 2 presents seasonal and annual long-term means of TCC, CLR, SCT, BKN, and OVC over SI and OW for the entire NBK in the period 1936–2013 and for three 20-yr periods, which represent three distinct temperature regimes: 1936–55, 1961–80, and 1993–2012. Figure 4 provides more detailed information on the year-to-year changes of cloudiness in the NBK, while Table 3 summarizes linear trends of cloudiness characteristics for the period 1936–2013 and for two halves of this period (1936–74 and 1975–2013) (supplementary Fig. S10 and Tables S3 and S4 provide similar information with the alternative accounting of cloud breaks).

Cloudiness shows both intra- and interannual variations. TCC has a minimum in winter in all three periods (over both SI and OW) and a maximum in summer or autumn (Table 2). CLR has a prominent annual cycle in all periods with the maximum in winter and the minimum in summer. SCT have little intra-annual variation over OW and in the annual cycle with winter maximum and summer minimum over SI (with the largest amplitude in the third period). Annual cycle of BKN became apparent only in the second period. In contrast, the annual cycle of OVC is distinctive, especially over SI where the summer maximum is 0.25–0.27 greater than the winter minimum. In general, the standard deviation is higher for CLR and OVC and for winter and autumn (Table 2).

Cloudiness over the entire NBK varies slightly from one period to another. In general, the first and the third periods are somewhat cloudier then the second (Table 2). The most pronounced changes are found in the autumn. In this season, NBK was noticeably cloudier in the first period over both OW and SI. For other seasons, the differences among the three periods do not exceed the standard deviation. Similar findings for TCC were obtained when using the alternative accounting of cloud breaks (Table S3).

Analysis of year-to-year changes of TCC revealed that the major long-term changes of TCC occurred in autumn (Fig. 4). TCC over SI dropped by more than 15% from the early twentieth century warming period to the end of the cool period of the 1970s–80s (from 82% in 1948 to 66% in 1987) (Fig. 4). Note that these changes exceed observation-related bias and can be treated as significant. The linear trend for autumnal TCC over SI for 1936–74 is also statistically significant (2% decade^{-1}) (Table 3). From the beginning of the 1990s autumnal TCC over SI started to increase; however, it is still less than it was in the 1940s. For other seasons, TCC over SI varies from year to year and displays no statistical trends, except for slight time changes in the period 1975–2013. A reduction of TCC over OW from the 1930s to the 1980s–90s, with a following increase, is found for summer and autumn (and to some extent for spring). In general, the 1940s was the cloudiest time over OW for all seasons, and the period 1936–74 was characterized by negative trends of TCC (significant for all seasons except summer) (Table 3). The period 1975–2013 was associated with positive and mostly insignificant trends of TCC over OW. All the observed changes and trends of TCC are qualitatively the same with those derived from the alternative accounting of cloud breaks (Fig. S10 and Table S4). In general, year-to-year changes of cloud characteristics in the entire NBK are the same for individual stations as well.

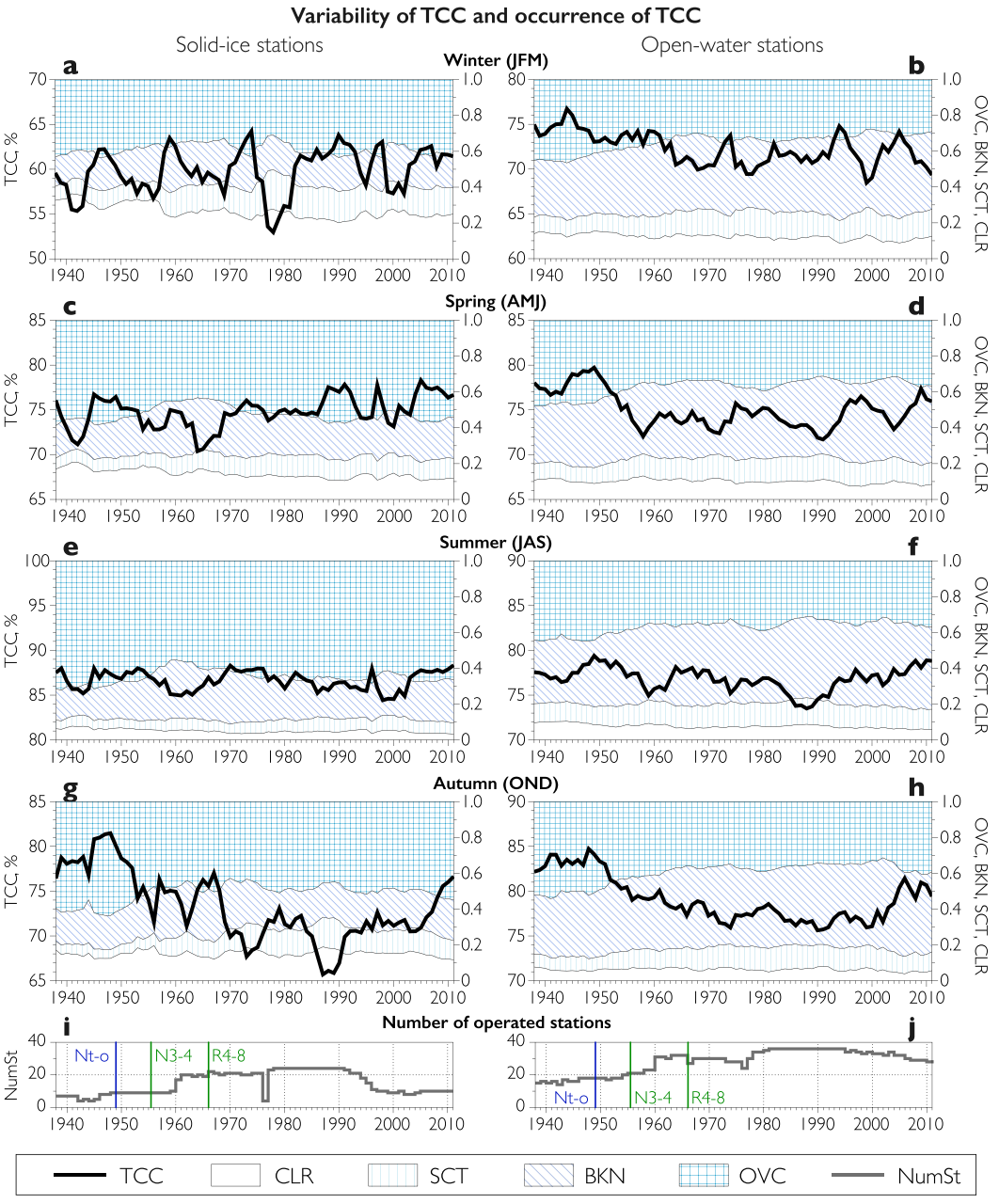

FIG. 4. Interannual variations of 5-yr running means of TCC, occurrence of reports with CLR, SCT, BKN, and OVC from 1938 to 2011 over the entire solid-ice (a),(c),(e),(g) and open-water (b),(d),(f),(h) regions of NBK for (a),(b) winter, (c),(d) spring, (e),(f) summer, and (g),(h) autumn. Cloud breaks are considered as 7 oktas, and reports with cloud breaks are considered as reports with broken clouds. Note that the absolute values for the left ordinate axis are different for different seasons (however, the range of 20% is kept for all seasons). Interannual variation of operated station number (NumSt) is shown for (i) solid-ice and (j) open-water parts of the NBK. The transition of Norwegian station from tenths to oktas (Nt-o) and the transitions of frequency of observations from 3 to 4 per day for Norwegian (N3–4) and from 4 to 8 per day for Russian station (R4–8) are marked.

TCC changes are consequences of mutual changes in CLR, SCT, BKN, and OVC (Tables 2 and S3; Figs. 4 and S9). CLR has a tendency for a steady decrease over both OW and SI. For instance, CLR in winter over SI has dropped from 0.30–0.35 at the beginning of the 1940s to 0.20–0.25 in the 2000s. In contrast, scattered clouds became more frequent in the NBK (mostly because of an increase from the 1940s to the 1990s). BKN has a strong,

TABLE 2. Cloudiness characteristics for the entire solid-ice and open-water regions of the NBK: mean values and standard deviations (in brackets). The first value is the total cloud cover (in %), and the other four values correspond to the frequencies of reports with clear sky, scattered clouds, broken clouds, and overcast, respectively. Cloud breaks are considered as 7 oktas, and reports with cloud breaks are considered as reports with broken clouds.

Season	1936–55	1961–80	1993–2012	1936–2013
		Solid-ice region		
Winter (JFM)	58 (6)	59 (6)	60 (4)	60 (5)
	0.34 (0.06)	0.26 (0.05)	0.25 (0.04)	0.27 (0.06)
	0.09 (0.02)	0.17 (0.04)	0.16 (0.02)	0.14 (0.04)
	0.17 (0.03)	0.22 (0.03)	0.20 (0.03)	0.20 (0.04)
	0.40 (0.06)	0.35 (0.06)	0.39 (0.06)	0.39 (0.06)
Spring (AMJ)	74 (4)	74 (4)	76 (3)	75 (4)
	0.18 (0.04)	0.14 (0.03)	0.12 (0.03)	0.15 (0.04)
	0.07 (0.01)	0.11 (0.02)	0.11 (0.02)	0.10 (0.03)
	0.19 (0.03)	0.27 (0.04)	0.23 (0.02)	0.23 (0.04)
	0.56 (0.04)	0.48 (0.05)	0.54 (0.04)	0.52 (0.05)
Summer (JAS)	87 (3)	87 (3)	87 (2)	87 (2)
	0.07 (0.03)	0.04 (0.02)	0.04 (0.01)	0.05 (0.02)
	0.06 (0.01)	0.07 (0.01)	0.07 (0.01)	0.06 (0.01)
	0.18 (0.03)	0.28 (0.05)	0.24 (0.03)	0.24 (0.05)
	0.69 (0.03)	0.61 (0.06)	0.65 (0.04)	0.65 (0.05)
Autumn (OND)	77 (6)	73 (6)	72 (3)	73 (6)
	0.16 (0.05)	0.15 (0.05)	0.15 (0.02)	0.15 (0.04)
	0.06 (0.02)	0.12 (0.03)	0.13 (0.02)	0.11 (0.04)
	0.19 (0.03)	0.26 (0.04)	0.23 (0.04)	0.23 (0.04)
	0.59 (0.07)	0.47 (0.07)	0.49 (0.05)	0.51 (0.08)
Whole year	74 (4)	73 (2)	74 (2)	73 (3)
	0.19 (0.04)	0.15 (0.02)	0.14 (0.02)	0.16 (0.03)
	0.07 (0.01)	0.11 (0.02)	0.12 (0.01)	0.10 (0.03)
	0.18 (0.02)	0.26 (0.04)	0.22 (0.02)	0.22 (0.04)
	0.56 (0.04)	0.48 (0.04)	0.52 (0.03)	0.52 (0.05)
		Open-water region		
Winter (JFM)	74 (3)	71 (3)	72 (4)	72 (4)
	0.14 (0.03)	0.12 (0.03)	0.11 (0.04)	0.12 (0.03)
	0.10 (0.02)	0.14 (0.02)	0.14 (0.02)	0.13 (0.03)
	0.33 (0.02)	0.41 (0.02)	0.44 (0.02)	0.40 (0.05)
	0.43 (0.04)	0.33 (0.04)	0.31 (0.04)	0.35 (0.06)
Spring (AMJ)	78 (2)	74 (2)	75 (3)	75 (3)
	0.11 (0.02)	0.11 (0.02)	0.08 (0.02)	0.10 (0.02)
	0.09 (0.01)	0.13 (0.01)	0.13 (0.01)	0.12 (0.02)
	0.35 (0.03)	0.41 (0.03)	0.44 (0.02)	0.40 (0.04)
	0.45 (0.04)	0.35 (0.03)	0.35 (0.03)	0.38 (0.05)
Summer (JAS)	78 (2)	77 (3)	77 (3)	77 (2)
	0.09 (0.02)	0.07 (0.02)	0.06 (0.02)	0.08 (0.02)
	0.11 (0.01)	0.13 (0.01)	0.12 (0.02)	0.12 (0.02)
	0.38 (0.03)	0.44 (0.03)	0.47 (0.03)	0.43 (0.04)
	0.42 (0.04)	0.36 (0.04)	0.35 (0.04)	0.37 (0.05)
Autumn (OND)	83 (3)	78 (2)	78 (4)	79 (4)
	0.06 (0.02)	0.07 (0.02)	0.06 (0.02)	0.06 (0.02)
	0.08 (0.02)	0.12 (0.01)	0.11 (0.02)	0.11 (0.03)
	0.36 (0.03)	0.44 (0.02)	0.47 (0.03)	0.43 (0.05)
	0.50 (0.05)	0.37 (0.02)	0.36 (0.04)	0.40 (0.07)
Whole year	78 (2)	75 (1)	76 (2)	76 (2)
	0.10 (0.01)	0.09 (0.01)	0.08 (0.02)	0.09 (0.02)
	0.09 (0.01)	0.13 (0.01)	0.13 (0.01)	0.12 (0.02)
	0.36 (0.02)	0.43 (0.02)	0.45 (0.02)	0.41 (0.04)
	0.45 (0.03)	0.35 (0.02)	0.34 (0.02)	0.38 (0.05)

statistically significant positive trend for the whole period (and for both halves) over OW in all seasons. BKN significantly increases from 0.30–0.34 at the end of the 1930s to 0.44–0.48 at the beginning of the 2000s (this increase exceeded the systematic bias). Over SI, the maximum of BKN was reached in the 1960s (around 0.3), and a statistically significant positive trend is noted for all seasons only for the period 1938–74 (Table 3). Changes of OVC are generally opposite to those for BKN. OVC over OW tends to decrease in all seasons, and it reduced from 0.45–0.5 in the 1930s to 0.3–0.35 in the 2000s (again, this decrease exceeds the systematic bias). Over SI, changes of OVC had two phases: a downward phase (present in all seasons) from the end of the 1930s to the end of the 1950s and an upward phase from the beginning of the 1960s to the present.

Another accounting of cloud breaks (Fig. S13; Table S4) does not qualitatively modify the reported changes in BKN and OVC over OW, but a notable difference is obtained over SI. Particularly, an almost monotonic increase of BKN and a decrease of OVC are found for all seasons.

5. Concluding remarks

We presented the long-term climatology of total cloud cover and the frequency of four conditions of cloud cover (clear sky, scattered clouds, broken clouds, and overcast) over the Norwegian, Barents, and Kara Seas based on surface observations at 15 Norwegian and 54 Russian weather stations divided into two broad regions with open-water and solid-ice conditions (OW and SI). The first cloud observations are from 1868. However, data for the end of the nineteenth century and the beginning of the twentieth century should be treated with caution because of their low quality and the presence of a number of shifts in time and procedure of observations. Thus, the main results were obtained for the period of 1936–2013.

Annual mean TCC in NBK is almost equal over SI and OW (73% ± 3% and 76% ± 2%, respectively). It is close to values obtained by Eastman and Warren (2010a) when surface stations and ship reports are combined (but for a shorter period) and 5%–10% less than was obtained from different satellite data for NBK (Chernokulsky and Mokhov 2012). TCC has a more pronounced annual cycle (over double the amplitude) over SI than over OW, with a minimum in the winter and a maximum in the summer (Table 2). Scattered clouds and clear skies are the least common types of cloud conditions, respectively, over SI and OW, while overcast and broken clouds are the most common types.

The analysis of long-term variability in TCC at individual stations and for the entire NBK region revealed a significant decrease in the middle of the twentieth century

TABLE 3. Linear trends of seasonal and annual means of total cloud cover (in % decade^{-1}) and the frequencies of clear sky, scattered clouds, broken clouds, and overcast (in parentheses; in decade$^{-1} \times 10^2$) for the entire solid-ice and open-water regions of the NBK for three periods: 1936–2013, 1936–74, and 1975–2013. Statistically significant values of the linear trend at the 0.1, 0.05, and 0.01 levels are shown with italics, bold italics, and bold, respectively. Cloud breaks are considered as 7 oktas, and reports with cloud breaks are considered as reports with broken clouds.

Season	1936–2013	1936–1974	1975–2013
		Solid-ice region	
Winter (JFM)	*0.5* (**−1.6**, ***1.3***, 0.2, 0.1)	1.1 (**−3.3**, **2.5**, ***2.5***, *−1.5*)	1.0 (0.2, ***−1.5***, −0.1, 1.4)
Spring (AMJ)	***0.5*** (**−1.2**, **0.8**, 0.3, 0.2)	0.1 (*−1.7*, **1.5**, ***3.8***, *−3.5*)	*0.8* (−0.6, −0.4, 0.2, 0.8)
Summer (JAS)	0.1 (**−0.5**, **0.3**, 0.6, −0.4)	0.4 (**−1.1**, 0.2, *4.4*, −3.4)	0.4 (−0.3, −0.2, −0.3, 0.7)
Autumn (OND)	***−0.9*** (−0.3, **1.5**, 0.3, ***−1.4***)	*−2.0* (−0.3, ***2.4***, ***3.1***, ***−5.1***)	0.5 (−0.2, −0.6, 0.6, 0.2)
Annual	0.0 (**−0.9**, ***1.0***, 0.4, −0.4)	−0.1 (***−1.6***, ***1.6***, *3.4*, *−3.4*)	*0.7* (−0.2, **−0.7**, 0.1, 0.8)
		Open-water region	
Winter (JFM)	***−0.5*** (**−0.5**, **0.8**, **1.8**, **−2.0**)	***−1.1*** (−0.6, **1.6**, *3.1*, **−4.0**)	0.1 (−0.4, −0.1, ***1.6***, *−1.1*)
Spring (AMJ)	*−0.4* (**−0.4**, **0.6**, **1.5**, **−1.6**)	***−1.6*** (0.2, **1.4**, ***3.0***, **−4.5**)	0.4 (−0.5, *−0.4*, *1.4*, −0.6)
Summer (JAS)	−0.1 (**−0.5**, ***0.3***, **1.5**, **−1.2**)	−0.2 (**−0.9**, **0.9**, *3.1*, **−2.9**)	***0.8*** (***−0.6***, **−0.7**, ***1.3***, 0.0)
Autumn (OND)	**−0.7** (−0.2, ***0.7***, **1.7**, **−2.2**)	**−2.2** (0.3, **1.9**, ***3.4***, **−5.4**)	0.6 (−0.2, **−0.9**, 0.9, 0.2)
Annual	**−0.4** (**−0.4**, *0.6*, *1.6*, ***−1.7***)	**−1.3** (−0.3, ***1.4***, 3.1, ***−4.2***)	0.5 (−0.4, ***−0.5***, 1.3, −0.4)

and an increase in the last few decades. These changes depend on season and region. Over SI, the minimum of TCC was distinguished in the 1960s in spring and in the late 1980s in autumn (Fig. 5). After the 1980s, TCC over SI increased (with a linear trend of around 3.0% decade^{-1}). This trend was also highlighted by Eastman and Warren (2010a). In general, over open-water regions, magnitudes of TCC trends are less than those over solid-ice regions, and the TCC minima are shifted to the end of the 1980s and beginning of the 1990s in most seasons. Both intra-annual and interannual variability of TCC are lower over OW stations compared to SI stations. The small changes of winter TCC in the last few decades come from a combination of the increase of winter TCC over the Norwegian and Barents Seas and the decrease over the Kara Sea. This decrease is in agreement with the negative trend of TCC obtained from merged ship- and station-based data (Eastman and Warren 2010a) and satellite observations

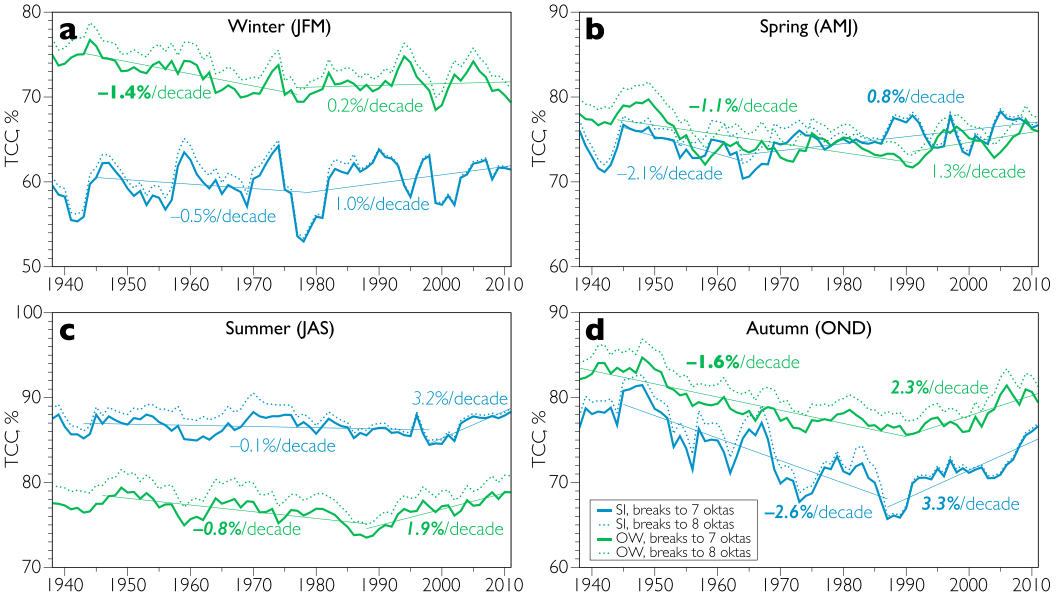

FIG. 5. Interannual variations of 5-yr running means of total cloud cover from 1938 to 2011 over the entire solid-ice (blue curves) and open-water (green curves) regions of the NBK for (a) winter, (b) spring, (c) summer, and (d) autumn. Cloud breaks are considered as 7 (solid lines) and 8 oktas (dashed lines). Linear regressions are shown for TCC when cloud breaks are considered as 7 oktas. Regressions counted for two periods: 1) from the maximum TCC in the early twentieth century warming to the absolute minimum (for the entire period) and 2) from this minimum to the last year. Italic, bold italic, and bold fonts indicate the confidence at the 0.1, 0.05, and 0.01 levels, respectively. Note that the absolute values for the ordinate axis are different for different seasons (however, the range of 30% is kept for all seasons).

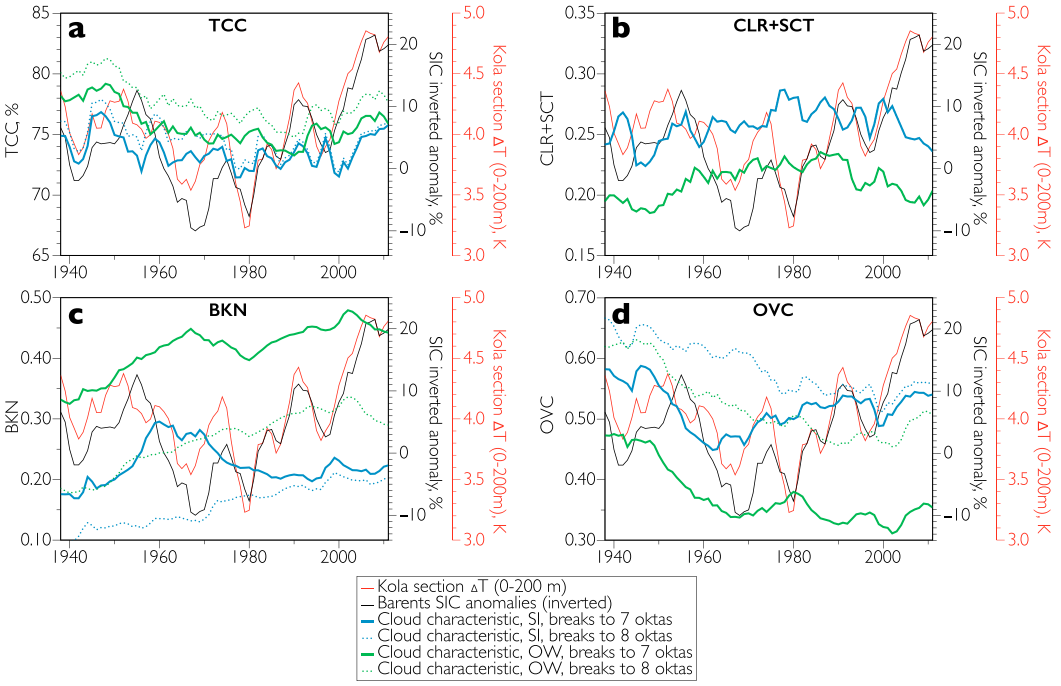

FIG. 6. Interannual variations of 5-yr running annual means of (a) TCC, (b) occurrence of reports with clear sky and scattered clouds (CLR + SCT), (c) BKN, and (d) OVC from 1938 to 2011 over the entire solid-ice (blue curves) and open-water (green curves) regions of the NBK. Cloud breaks are considered as 7 (solid lines) and 8 oktas (dashed lines); reports with cloud breaks are considered as reports with broken clouds (solid lines) or overcast (dashed lines). Note that the absolute values for the left ordinate axis are different for different cloud characteristics. The red line shows the 5-yr running annual means of ocean temperature between 0- and 200-m depth in the Kola section (data from the Polar Research Institute of Marine Fisheries and Oceanography, Russia; Karsakov 2009). The gray line shows the 5-yr running annual means of inverted annual mean Barents Sea ice coverage anomalies [data adopted from Zhichkin (2015)].

(Liu et al. 2007). Our results do not show a decrease of TCC (with the corresponding increase of CLR) in spring over the eastern NBK as was found by Eastman and Warren (2010a); however, these results cannot be compared directly because of a different averaging procedure, different seasons assessed, and different region divisions with different numbers of stations used.

Arctic cloud formation and evolution are markedly affected by surface properties, primarily sea ice concentration (Eastman and Warren 2010a; Palm et al. 2010; Sato et al. 2012; Liu et al. 2012b). A mutual interannual variability of sea ice concentration (SIC) in the Barents Sea with associated cloud changes in NBK was found for the twentieth century (Fig. 6). Thus, the maximum of SIC in the Barents Sea and the minimum of temperature from the Kola section $\Delta T_{\mathrm{Kola,0–200m}}$ (the measure of Atlantic warm water inflow into the Barents Sea) is found in the 1960s–80s, which coincides with the minimum of TCC and the maximum of the combined CLR and SCT conditions (Figs. 6a,b) over SI stations. The correlation coefficient between the annual mean SIC ($\Delta T_{\mathrm{Kola,0–200m}}$) and TCC over SI equals −0.38 (0.44) and is statistically significant (at the 0.01 level). Over OW stations, an overall increase in the frequency of broken cloud conditions and a decrease in the frequency of overcast conditions were found (Figs. 6c,d). These changes are likely connected with long-term changes of morphological types in NBK: an increase (decrease) of amount of convective (stratiform) clouds (supplementary Figs. S10–12) (Esau and Chernokulsky 2015). However, cloudiness over OW shows nonsignificant correlation with SIC and T_{Kola}.

Various authors have suggested different mechanisms for cloud–sea ice relationships. One proposed mechanism is that a reduction of summer and autumn sea ice may lead to an increase of cloudiness in autumn (Eastman and Warren 2010a; Palm et al. 2010; Sato et al. 2012). Another mechanism is that the clouds themselves may influence sea ice properties. Specifically, it is proposed that changes of clouds in the first half of the year modulate shortwave (Kay et al. 2008; Kay and Gettelman 2009; Choi et al. 2014) or longwave (Kapsch et al. 2013, Liu and Key 2014; Letterly et al. 2016) radiative fluxes and therefore determine sea ice

concentrations during its intra-annual minimum (August–September). Our dataset of long-term observations for clouds will help to better evaluate this kind of relationship. For instance, strong positive correlation of spring and autumn TCC (with correlation coefficient of 0.49 for OW) (supplementary Fig. S14) indicates their closely tied relationship, presumably through modulating sea ice. Additional studies are required to robustly establish this finding.

Acknowledgments. We appreciate three anonymous reviewers for many constructive and efficient comments. We thank Ryan Eastman for providing the routine for computing the moonlight criterion. The Kola section data were provided by the Polar Research Institute of Marine Fisheries and Oceanography (PINRO; http://www.pinro.ru), and eKlima data were obtained from the Norwegian Meteorological Institute (http://eklima.no). The research was supported by the Russian Science Foundation (Project 14-17-00647). Additional support for data processing was received from the RF President Grant MK-4513.2016.5, from NORRUSS CLIMARC project (Climate variability and Change in the Eurasian Arctic in the 21st Century), and from the RFBR and RAS programs. I. Esau and R. Davy were supported by the Bjerknes Centre for Climate Research project BASIC: Boundary Layers in the Arctic Atmosphere, Seas and Ice Dynamics.

REFERENCES

Akperov, M., I. Mokhov, A. Rinke, K. Dethloff, and H. Matthes, 2015: Cyclones and their possible changes in the Arctic by the end of the twenty first century from regional climate model simulations. *Theor. Appl. Climatol.*, **122**, 85–96, doi:10.1007/s00704-014-1272-2.

Bartlett, M. S., 1935: Some aspects of the time-correlation problem in regard to tests of significance. *J. Roy. Stat. Soc.*, **98**, 536–543.

Bednorz, E., D. Kaczmarek, and P. Dudlik, 2016: Atmospheric conditions governing anomalies of the summer and winter cloudiness in Spitsbergen. *Theor. Appl. Climatol.*, **123**, 1–10, doi:10.1007/s00704-014-1326-5.

Bekryaev, R. V., I. V. Polyakov, and V. A. Alexeev, 2010: Role of polar amplification in long-term surface air temperature variations and modern Arctic warming. *J. Climate*, **23**, 3888–3906, doi:10.1175/2010JCLI3297.1.

Bengtsson, L., V. A. Semenov, and O. M. Johannesen, 2004: The early twentieth-century warming in the Arctic—A possible mechanism. *J. Climate*, **17**, 4045–4057, doi:10.1175/1520-0442(2004)017<4045:TETWIT>2.0.CO;2.

Brümmer, B., and S. Pohlmann, 2000: Wintertime roll and cell convection over Greenland and Barents Sea regions: A climatology. *J. Geophys. Res.*, **105**, 15 559–15 566, doi:10.1029/1999JD900841.

Bulygina, O. N., V. M. Veselov, V. N. Razuvaev, and T. M. Aleksandrova, 2014: Three-hourly meteorological observations from Russian meteorological stations. [Available online at http://meteo.ru/english/climate/descrip12.htm.]

Chernokulsky, A., and I. I. Mokhov, 2010: Intercomparison of global and zonal cloudiness characteristics from different satellite and ground-based data (in Russian). *Issledovania Zemli iz Kosmosa*, **3**, 12–29.

——, and ——, 2012: Climatology of total cloudiness in the Arctic: An intercomparison of observations and reanalyses. *Adv. Meteor.*, **2012**, 542093, doi:10.1155/2012/542093.

——, O. N. Bulygina, and I. I. Mokhov, 2011: Recent variations of cloudiness over Russia from surface daytime observations. *Environ. Res. Lett.*, **6**, 035202, doi:10.1088/1748-9326/6/3/035202.

——, I. I. Mokhov, and N. Nikitina, 2013: Winter cloudiness variability over northern Eurasia related to the Siberian High during 1966–2010. *Environ. Res. Lett.*, **8**, 045012, doi:10.1088/1748-9326/8/4/045012.

Choi, Y. S., B. M. Kim, S. K. Hur, and S. J. Kim, 2014: Connecting early summer cloud-controlled sunlight and late summer sea ice in the Arctic. *J. Geophys. Res. Atmos.*, **119**, 11 087–11 099, doi:10.1002/2014JD022013.

Curry, J. A., W. B. Rossow, D. Randall, and J. L. Schramm, 1996: Overview of Arctic cloud and radiation characteristics. *J. Climate*, **9**, 1731–1764, doi:10.1175/1520-0442(1996)009<1731:OOACAR>2.0.CO;2.

Czernecki, B., M. Taszarek, L. Kolendowicz, and K. Szyga-Pluta, 2013: Atmospheric conditions of thunderstorms in the European part of the Arctic derived from sounding and reanalysis data. *Atmos. Res.*, **154**, 60–72, doi:10.1016/j.atmosres.2014.11.001.

Eastman, R., and S. G. Warren, 2010a: Interannual variations of Arctic cloud types in relation to sea ice. *J. Climate*, **23**, 4216–4232, doi:10.1175/2010JCLI3492.1.

——, and ——, 2010b: Arctic cloud changes from surface and satellite observations. *J. Climate*, **23**, 4233–4242, doi:10.1175/2010JCLI3544.1.

——, and ——, 2013: A 39-yr survey of cloud changes from land stations worldwide 1971–2009: Long-term trends, relation to aerosols, and expansion of the tropical belt. *J. Climate*, **26**, 1286–1303, doi:10.1175/JCLI-D-12-00280.1.

——, and ——, 2014: Diurnal cycles of cumulus, cumulonimbus, stratus, stratocumulus, and fog from surface observations over land and ocean. *J. Climate*, **27**, 2386–2404, doi:10.1175/JCLI-D-13-00352.1.

——, ——, and C. J. Hahn, 2011: Variations in cloud cover and cloud types over the ocean from surface observations, 1954–2008. *J. Climate*, **24**, 5914–5934, doi:10.1175/2011JCLI3972.1.

English, J. M., A. Gettelman, and G. R. Henderson, 2015: Arctic radiative fluxes: Present-day biases and future projections in CMIP5 models. *J. Climate*, **28**, 6019–6038, doi:10.1175/JCLI-D-14-00801.1.

Esau, I. N., and A. V. Chernokulsky, 2015: Convective cloud fields in the Atlantic sector of the Arctic: Satellite and ground-based observations. *Izv., Atmos. Ocean. Phys.*, **51**, 1007–1020, doi:10.1134/S000143381509008X.

Francis, J. A., and E. Hunter, 2007: Changes in the fabric of the Arctic's greenhouse blanket. *Environ. Res. Lett.*, **2**, 045011, doi:10.1088/1748-9326/2/4/045011.

Free, M., and B. Sun, 2013: Time-varying biases in U.S. total cloud cover data. *J. Atmos. Oceanic Technol.*, **30**, 2838–2849, doi:10.1175/JTECH-D-13-00026.1.

Hahn, C. J., and S. G. Warren, 2007: A gridded climatology of clouds over land (1971–96) and ocean (1954–97) from surface observations worldwide. Carbon Dioxide Information Analysis Center, Oak Ridge National Laboratory, Numeric Data Product NDP-026E, 71 pp. [Available online at http://cdiac.ornl.gov/epubs/ndp/ndp026e/ndp026e.html.]

——, ——, and J. London, 1995: The effect of moonlight on observation of cloud cover at night, and application to cloud climatology. *J. Climate*, **8**, 1429–1446, doi:10.1175/1520-0442(1995)008<1429:TEOMOO>2.0.CO;2.

Heintzenberg, J., C. Leck, and P. Tunved, 2015: Potential source regions and processes of aerosol in the summer Arctic. *Atmos. Chem. Phys.*, **15**, 6487–6502, doi:10.5194/acp-15-6487-2015.

Henderson-Sellers, A., 1992: Continental cloudiness changes this century. *GeoJournal*, **27**, 255–262, doi:10.1007/BF02482666.

Herman, G., and R. Goody, 1976: Formation and persistence of summertime Arctic stratus clouds. *J. Atmos. Sci.*, **33**, 1537–1553, doi:10.1175/1520-0469(1976)033<1537:FAPOSA>2.0.CO;2.

Jiang, J. H., and Coauthors, 2012: Evaluation of cloud and water vapor simulations in CMIP5 climate models using NASA "A-Train" satellite observations. *J. Geophys. Res.*, **117**, D14105, doi:10.1029/2011JD017237.

Kapsch, M.-L., R. G. Graversen, and M. Tjernström, 2013: Springtime atmospheric energy transport and the control of Arctic summer sea-ice extent. *Nat. Climate Change*, **3**, 744–748, doi:10.1038/nclimate1884.

Karlsson, J., and G. Svensson, 2013: Consequences of poor representation of Arctic sea-ice albedo and cloud-radiation interactions in the CMIP5 model ensemble. *Geophys. Res. Lett.*, **40**, 4374–4379, doi:10.1002/grl.50768.

Karlsson, K. G., and Coauthors, 2013: CLARA-A1: A cloud, albedo, and radiation dataset from 28 yr of global AVHRR data. *Atmos. Chem. Phys.*, **13**, 5351–5367, doi:10.5194/acp-13-5351-2013.

Karsakov, A. L., 2009: Oceanographical research in the Kola section in the Barents Sea for the period 1900–2008. Polar Research Institute of Marine Fisheries and Oceanography Rep., 139 pp.

Kay, J. E., and A. Gettelman, 2009: Cloud influence on and response to seasonal Arctic sea ice loss. *J. Geophys. Res.*, **114**, D18204, doi:10.1029/2009JD011773.

——, T. S. L'Ecuyer, A. Gettelman, G. L. Stephens, and C. O'Dell, 2008: The contribution of cloud and radiation anomalies to the 2007 Arctic sea ice extent minimum. *Geophys. Res. Lett.*, **35**, L08503, doi:10.1029/2008GL033451.

King, M. D., S. Platnick, W. P. Menzel, S. A. Ackerman, and P. A. Hubanks, 2013: Spatial and temporal distribution of clouds observed by MODIS onboard the Terra and Aqua satellites. *IEEE Trans. Geosci. Remote Sens.*, **51**, 3826–3852, doi:10.1109/TGRS.2012.2227333.

Kolstad, E. W., T. J. Bracegirdle, and I. A. Seierstad, 2009: Marine cold-air outbreaks in the North Atlantic: Temporal distribution and associations with large-scale atmospheric circulation. *Climate Dyn.*, **33**, 187–197, doi:10.1007/s00382-008-0431-5.

Komurcu, M., and Coauthors, 2014: Intercomparison of the cloud water phase among global climate models. *J. Geophys. Res. Atmos.*, **119**, 3372–3400, doi:10.1002/2013JD021119.

Letterly, A., J. Key, and Y. Liu, 2016: The influence of winter cloud on summer sea ice in the Arctic, 1983–2013. *J. Geophys. Res. Atmos.*, **121**, 2178–2187, doi:10.1002/2015JD024316.

Li, J., J. Huang, K. Stamnes, T. Wang, Q. Lv, and H. Jin, 2015: A global survey of cloud overlap based on CALIPSO and CloudSat measurements. *Atmos. Chem. Phys.*, **15**, 519–536, doi:10.5194/acp-15-519-2015.

Li, J. L. F., and Coauthors, 2012: An observationally based evaluation of cloud ice water in CMIP3 and CMIP5 GCMs and contemporary reanalyses using contemporary satellite data. *J. Geophys. Res.*, **117**, D16105, doi:10.1029/2012JD017640.

Lindsay, R., M. Wensnahan, A. Schweiger, and J. Zhang, 2014: Evaluation of seven different atmospheric reanalysis products in the Arctic. *J. Climate*, **27**, 2588–2606, doi:10.1175/JCLI-D-13-00014.1.

Liu, Y., and J. R. Key, 2014: Less winter cloud aids summer 2013 Arctic sea ice return from 2012 minimum. *Environ. Res. Lett.*, **9**, 044002, doi:10.1088/1748-9326/9/4/044002.

——, and ——, 2016: Assessment of Arctic cloud cover anomalies in atmospheric reanalysis products using satellite data. *J. Climate*, **29**, 6065–6083, doi:10.1175/JCLI-D-15-0861.1.

——, ——, J. A. Francis, and X. Wang, 2007: Possible causes of decreasing cloud cover in the Arctic winter, 1982–2000. *Geophys. Res. Lett.*, **34**, L14705, doi:10.1029/2007GL030042.

——, ——, and X. Wang, 2008: The influence of changes in cloud cover on recent surface temperature trends in the Arctic. *J. Climate*, **21**, 705–715, doi:10.1175/2007JCLI1681.1.

——, ——, S. A. Ackerman, G. G. Mace, and Q. Zhang, 2012a: Arctic cloud macrophysical characteristics from CloudSat and CALIPSO. *Remote Sens. Environ.*, **124**, 159–173, doi:10.1016/j.rse.2012.05.006.

——, ——, Z. Liu, X. Wang, and S. J. Vavrus, 2012b: A cloudier Arctic expected with diminishing sea ice. *Geophys. Res. Lett.*, **39**, L05705, doi:10.1029/2012GL051251.

Mace, G. G., Q. Zhang, M. Vaughan, R. Marchand, G. Stephens, C. Trepte, and D. Winker, 2009: A description of hydrometeor layer occurrence statistics derived from the first year of merged CloudSat and CALIPSO data. *J. Geophys. Res.*, **114**, D00A26, doi:10.1029/2007JD009755.

Mokhov, I. I., 1991: Trends of global and polar cloudiness from satellite data. *Proc. Int. Conf. on the Role of the Polar Regions in Global Change*, Fairbanks, AK, University of Alaska Fairbanks, 176–182.

——, and M. E. Schlesinger, 1993: Analysis of global cloudiness: 1. Comparison of Meteor, Nimbus 7, and International Satellite Cloud Climatology Project (ISCCP) satellite data. *J. Geophys. Res.*, **98**, 12 849–12 868, doi:10.1029/93JD00530.

——, and ——, 1994: Analysis of global cloudiness: 2. Comparison of ground-based and satellite-based cloud climatologies. *J. Geophys. Res.*, **99**, 17 045–17 065, doi:10.1029/94JD00943.

——, A. V. Chernokul'skii, M. G. Akperov, J.-L. Dufresne, and H. Le Treut, 2009: Variations in the characteristics of cyclonic activity and cloudiness in the atmosphere of extratropical latitudes of the Northern Hemisphere based from model calculations compared with the data of the reanalysis and satellite data. *Dokl. Earth Sci.*, **424**, 147–150, doi:10.1134/S1028334X09010310.

Okland, H., 1987: Heating by organized convection as a source of polar low intensification. *Tellus*, **39A**, 397–407, doi:10.1111/j.1600-0870.1987.tb00317.x.

Outten, S., and I. Esau, 2012: A link between Arctic sea ice and recent cooling trends over Eurasia. *Climatic Change*, **110**, 1069–1075, doi:10.1007/s10584-011-0334-z.

Palm, S. P., S. T. Strey, J. Spinhirne, and T. Markus, 2010: Influence of Arctic sea ice extent on polar cloud fraction and vertical structure and implications for regional climate. *J. Geophys. Res.*, **115**, D21209, doi:10.1029/2010JD013900.

Petoukhov, V., and V. A. Semenov, 2010: A link between reduced Barents-Kara sea ice and cold winter extremes over northern continents. *J. Geophys. Res.*, **115**, D21111, doi:10.1029/2009JD013568.

Pithan, F., and T. Mauritsen, 2014: Arctic amplification dominated by temperature feedbacks in contemporary climate models. *Nat. Geosci.*, **7**, 181–184, doi:10.1038/ngeo2071.

Previdi, M., and D. E. Veron, 2007: North Atlantic cloud cover response to the North Atlantic oscillation and relationship to surface temperature changes. *J. Geophys. Res.*, **112**, D07104, doi:10.1029/2006JD007516.

Przybylak, R., 1999: Influence of cloudiness on extreme air temperatures and diurnal temperature range in the Arctic in 1951–1990. *Pol. Polar Res.*, **20**, 149–173.

Raatz, W. E., 1981: Trends in cloudiness in the Arctic since 1920. *Atmos. Environ.*, **15**, 1503–1506, doi:10.1016/0004-6981(81)90358-9.

Rayner, N. A., D. E. Parker, E. D. Horton, C. L. Folland, L. V. Alexander, D. P. Rowell, E. C. Kent, and A. Kaplan, 2003: Global analyses of sea surface temperature, sea ice, and night marine air temperature since the late nineteenth century. *J. Geophys. Res.*, **108**, 4407, doi:10.1029/2002JD002670.

Sato, K., J. Inoue, Y.-M. Kodama, and J. E. Overland, 2012: Impact of Arctic sea-ice retreat on the recent change in cloud-base height during autumn. *Geophys. Res. Lett.*, **39**, L10503, doi:10.1029/2012GL051850.

Semenov, V. A., and M. Latif, 2015: Nonlinear winter atmospheric circulation response to Arctic sea ice concentration anomalies for different periods during 1966–2012. *Environ. Res. Lett.*, **10**, 054020, doi:10.1088/1748-9326/10/5/054020.

Serreze, M. C., and R. G. Barry, 2011: Processes and impacts of Arctic amplification: A research synthesis. *Global Planet. Change*, **77**, 85–96, doi:10.1016/j.gloplacha.2011.03.004.

Shupe, M. D., and J. M. Intrieri, 2004: Cloud radiative forcing of the Arctic surface: The influence of cloud properties, surface albedo, and solar zenith angle. *J. Climate*, **17**, 616–628, doi:10.1175/1520-0442(2004)017<0616:CRFOTA>2.0.CO;2.

Smedsrud, L. H., and Coauthors, 2013: The role of the Barents Sea in the Arctic climate system. *Rev. Geophys.*, **51**, 415–449, doi:10.1002/rog.20017.

Stanhill, G., 1995: Solar irradiance, air pollution and temperature changes in the Arctic. *Philos. Trans. Roy. Soc. London*, **352A**, 247–258, doi:10.1098/rsta.1995.0068.

Stubenrauch, C. J., and Coauthors, 2013: Assessment of global cloud datasets from satellites: Project and database initiated by the GEWEX Radiation Panel. *Bull. Amer. Meteor. Soc.*, **94**, 1031–1049, doi:10.1175/BAMS-D-12-00117.1.

Taylor, P. C., M. Cai, A. Hu, J. Meehl, W. Washington, and G. J. Zhang, 2013: A decomposition of feedback contributions to polar warming amplification. *J. Climate*, **26**, 7023–7043, doi:10.1175/JCLI-D-12-00696.1.

Vavrus, S., U. S. Bhatt, and V. A. Alexeev, 2011a: Factors influencing simulated changes in future Arctic cloudiness. *J. Climate*, **24**, 4817–4830, doi:10.1175/2011JCLI4029.1.

——, M. M. Holland, and D. A. Bailey, 2011b: Changes in Arctic clouds during intervals of rapid sea ice loss. *Climate Dyn.*, **36**, 1475–1489, doi:10.1007/s00382-010-0816-0.

Wang, X., and J. R. Key, 2005a: Arctic surface, cloud, and radiation properties based on the AVHRR polar pathfinder dataset. Part I: Spatial and temporal characteristics. *J. Climate*, **18**, 2558–2574, doi:10.1175/JCLI3438.1.

——, and ——, 2005b: Arctic surface, cloud, and radiation properties based on the AVHRR polar pathfinder dataset. Part II: Recent trends. *J. Climate*, **18**, 2575–2593, doi:10.1175/JCLI3439.1.

Warren, S. G., R. Eastman, and C. J. Hahn, 2007: A survey of changes in cloud cover and cloud types over land from surface observations, 1971–96. *J. Climate*, **20**, 717–738, doi:10.1175/JCLI4031.1.

Wood, R., 2012: Stratocumulus clouds. *Mon. Wea. Rev.*, **140**, 2373–2423, doi:10.1175/MWR-D-11-00121.1.

——, and P. R. Field, 2011: The distribution of cloud horizontal sizes. *J. Climate*, **24**, 4800–4816, doi:10.1175/2011JCLI4056.1.

Wylie, D., 2008: Diurnal cycles of clouds and how they affect polar-orbiting satellite data. *J. Climate*, **21**, 3989–3996, doi:10.1175/2007JCLI2027.1.

Zhang, X., J. He, J. Zhang, I. V. Polyakov, R. Gerdes, J. Inoue, and P. Wu, 2012: Enhanced poleward moisture transport and amplified northern high-latitude wetting trend. *Nat. Climate Change*, **3**, 47–51, doi:10.1038/nclimate1631.

Zhichkin, A. P., 2015: Peculiarities of interannual and seasonal variations of the Barents Sea ice coverage anomalies. *Russ. Meteor. Hydrol.*, **40**, 319–326, doi:10.3103/S1068373915050052.